

# PROJECT 5: Signal Processing

TASK 5.1: Signal and Image Processing

PI:

Aleksandar Dogandžić

STUDENT:

Renliang Gu



## OBJECTIVE:

Develop methods for detecting defects and estimating their properties (e.g., size, shape, and orientation) from noisy measurements collected using a single or multiple NDE inspection modalities.

## TOPICS:

- Defect detection,
- Parametric flaw modeling,
- System design and performance analysis,
- Data fusion,
- Statistical characterization of flaw signals,
- Sparse signal reconstruction.

# RELATIONSHIP TO UTOPIAN VIEW:

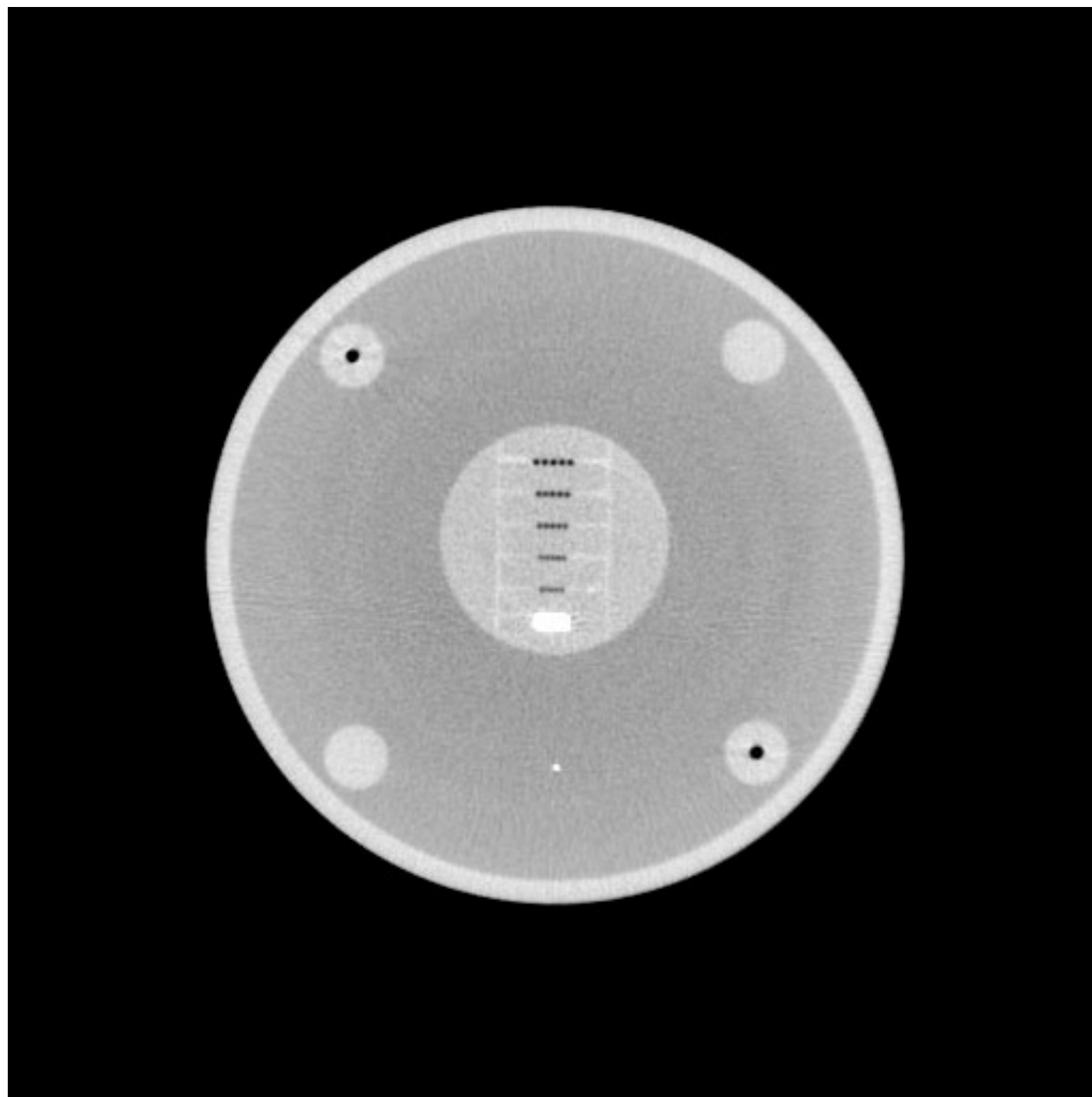
Applying sparse signal reconstruction and compressive sampling to NDE has potential for

- successfully handling ill-posed problems due to limited-angle projections, and therefore achieving *better* reconstruction performance than the standard approaches that ignore signal sparsity, and
- providing *faster* and therefore *cheaper* inspections compared with the existing methods.

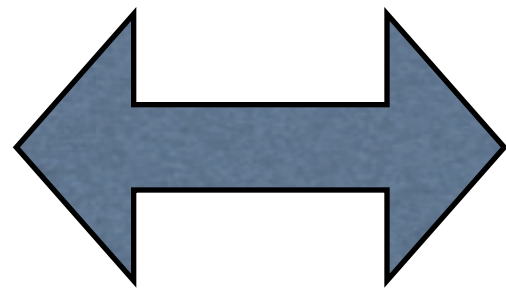
# Outline

- Background.
- Measurement Model and Mask Reconstruction Algorithms for Known Object Contour.
- Automatic Mask Generation from X-ray CT Sinograms Using a Convex Hull of the Object.
- Numerical Examples
  - Shepp-Logan phantom reconstruction,
  - Industrial object reconstruction.

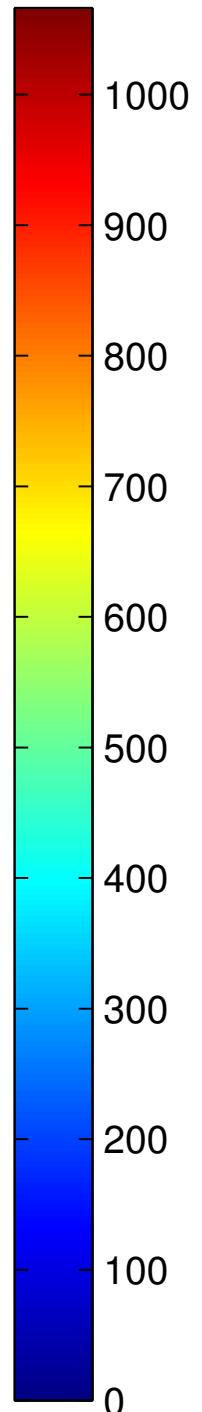
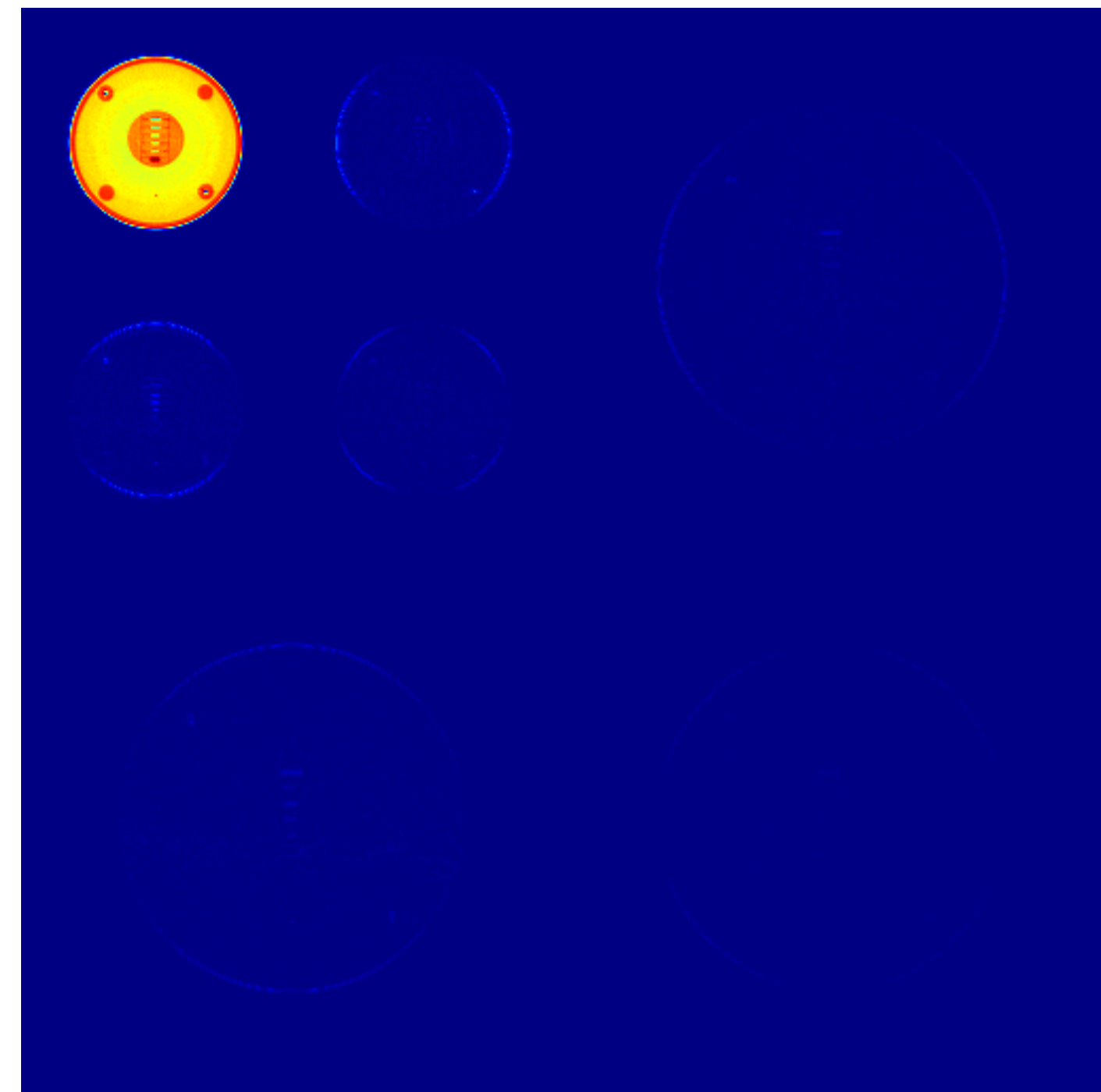
# Signal Sparsity



transform



DWT



$\underline{x}$   
signal

$\underline{\Psi}$   
sparsifying  
transform matrix

$\underline{s}$   
sparse signal  
transform-coefficient vector

# Geometric Object Information

We incorporate the geometric constraints via the following signal model: the elements of the  $p \times l$  signal vector  $\mathbf{x} = [x_1, x_2, \dots, x_p]^T$  are

$$x_i = \begin{cases} [\Psi s]_i, & i \in M \\ 0, & i \notin M \end{cases}, \quad i = 1, 2, \dots, p$$

where the mask  $M$  is the set of  $p_M \times p$  indices corresponding to the signal elements inside the contour of the inspected object and  $\Psi$  is the known orthogonal sparsifying transform matrix.

# Our Mask Measurement Model

We model the  $N \times l$  vector of X-ray CT measurements as

$$\begin{bmatrix} y \\ \end{bmatrix}_{N \times 1} = \begin{bmatrix} \text{sampling operator} \\ \Phi_{:,M} \text{ of size } N \times p_M \end{bmatrix} \quad \begin{bmatrix} \text{subset of } \Psi_M \\ \Psi_{M,I} \text{ of size } p_M \times p_I \end{bmatrix} \quad \begin{bmatrix} s_I \\ \end{bmatrix}_{p_I \times 1}$$

i.e.

$$y = H s_I$$

where

- $s_I$  is the  $p_I \times l$  vector of identifiable signal transform coefficients and
- $H = \Phi_{:,M} \Psi_{M,I}$  is the  $N \times p_I$  *sensing matrix*.

# Our Mask Reconstruction Algorithms

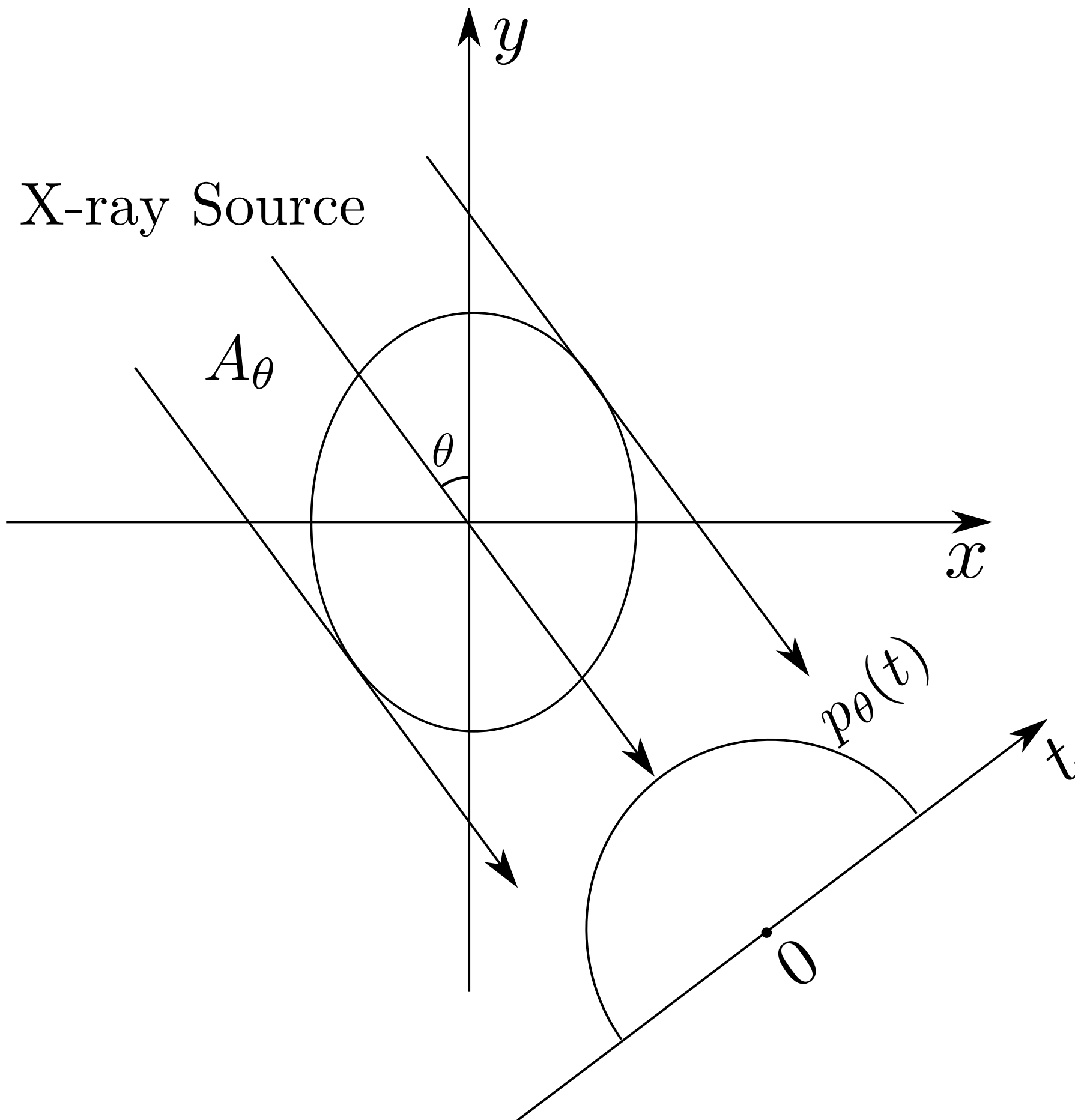
- Mask iterative hard thresholding algorithms (mask IHT and mask DORE) that aim at solving

$$(P_0) : \min_{\mathbf{s}_I} \|y - H \mathbf{s}_I\|_2^2 \quad \text{subject to } \|\mathbf{s}_I\|_0 \leq r$$

- Mask convex relaxation algorithms (mask FPC and mask GPSR) for solving

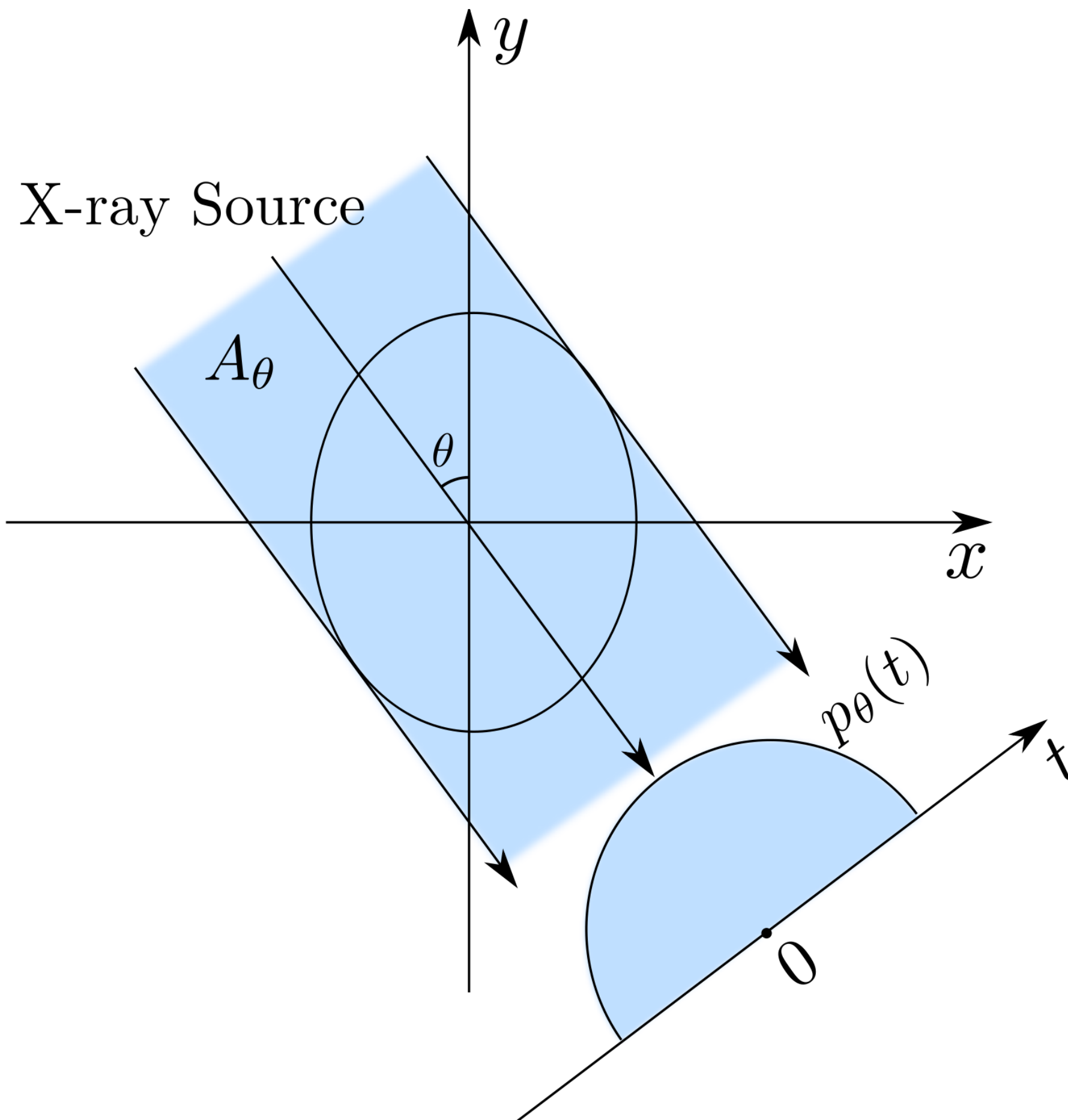
$$(P_1) : \min_{\mathbf{s}_I} \left( \frac{1}{2} \|y - H \mathbf{s}_I\|_2^2 + \tau \|\mathbf{s}_I\|_1 \right)$$

# Geometry of Parallel-beam X-ray CT System



Denote the measured sinogram by  $p_\theta(t)$ , where  $\theta$  is the projection angle and  $t$  is the distance from the rotation center  $O$  to the measurement point.

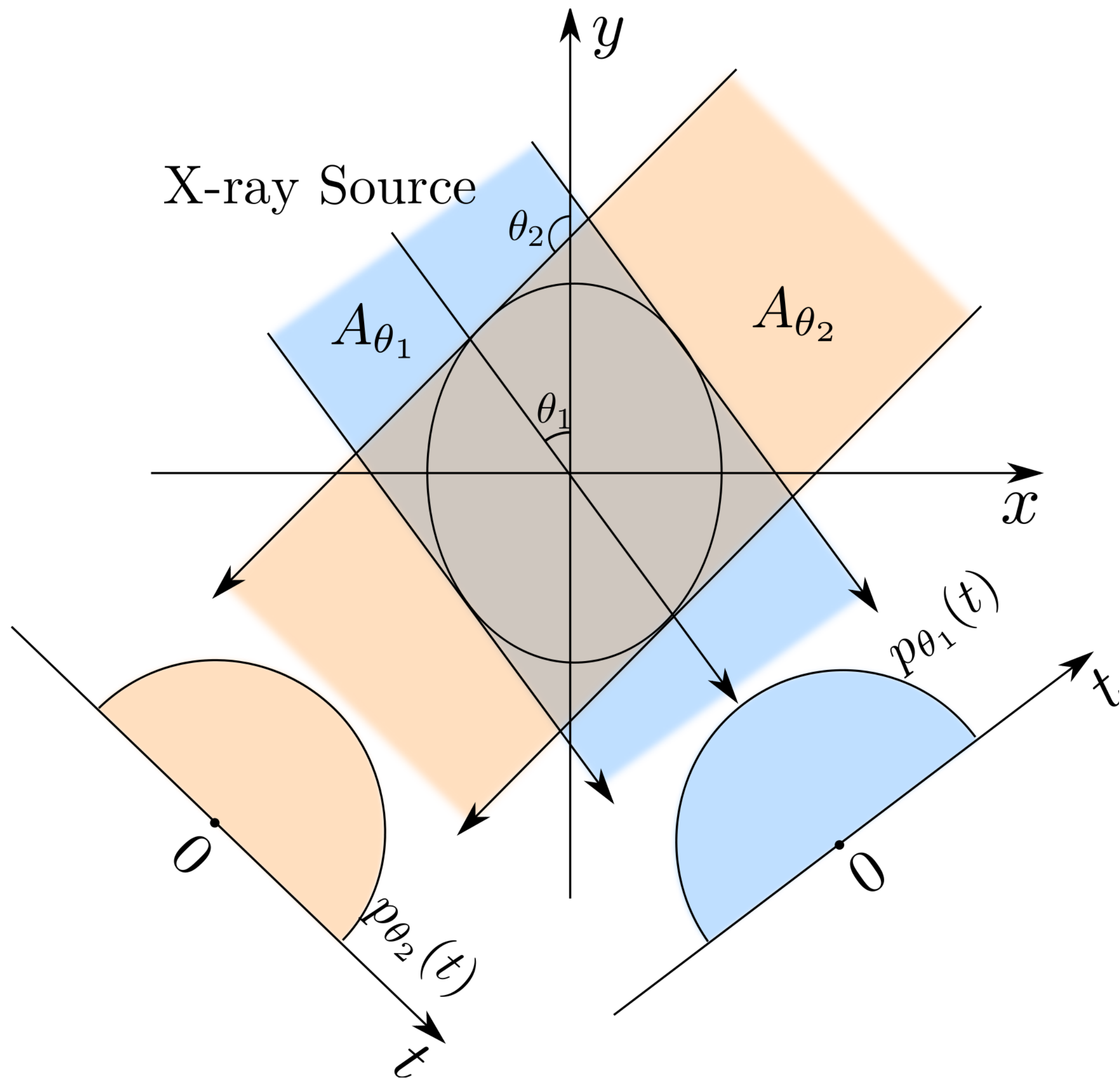
# Geometry of Parallel-beam X-ray CT System



Define the range of the sinogram at angle  $\theta$  by  $[a_\theta, b_\theta] = \inf \{[a, b] \in R : p_\theta(t) = 0 \text{ for all } t \notin [a, b]\}$  and the corresponding range in the spatial image

$$A_\theta = \{(x, y) \in \mathbb{R}^2 : x \cos \theta + y \sin \theta \in [a_\theta, b_\theta]\}$$

# Convex Hull Construction

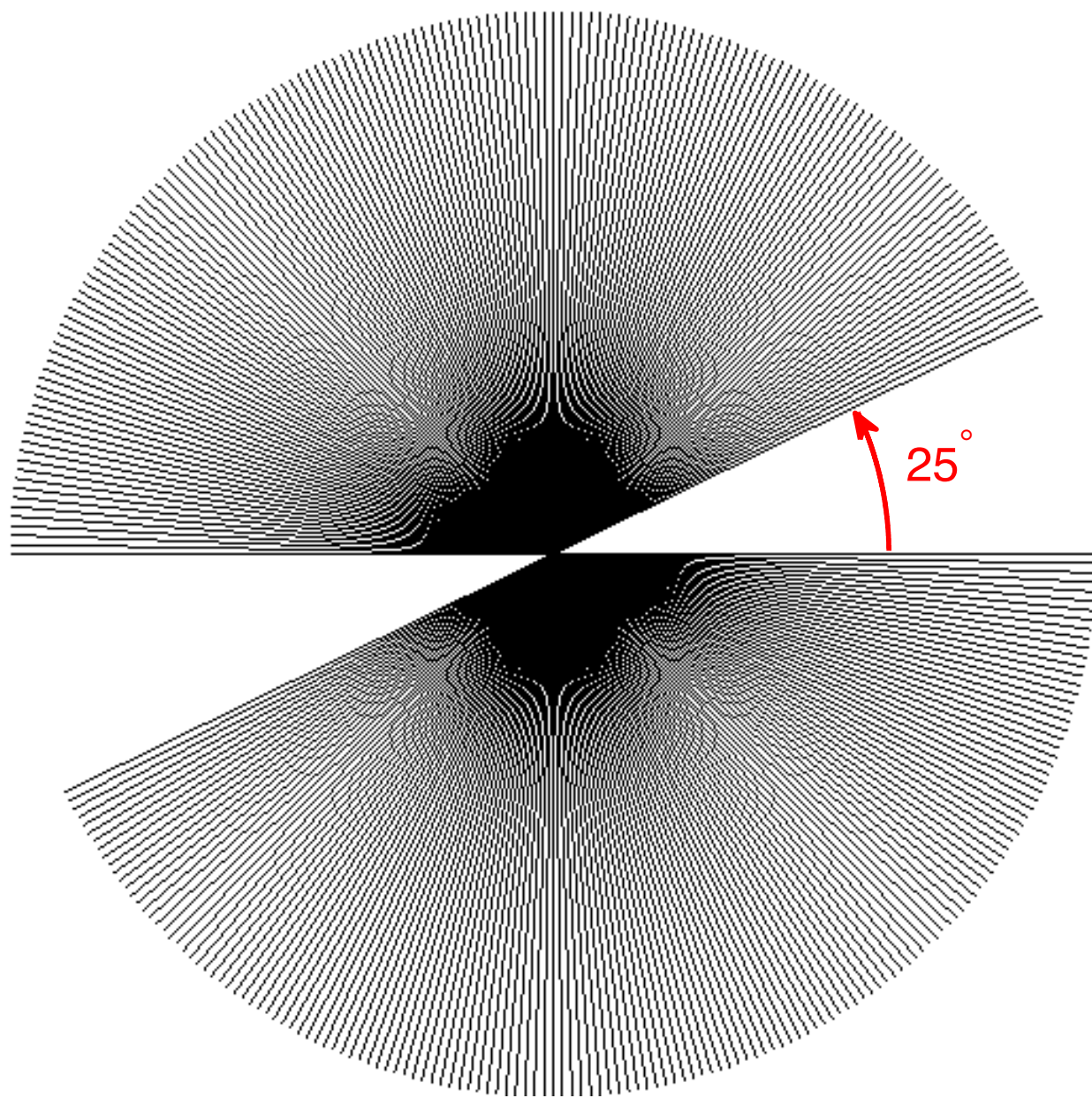


Construct the convex hull of the inspected object by taking the intersection

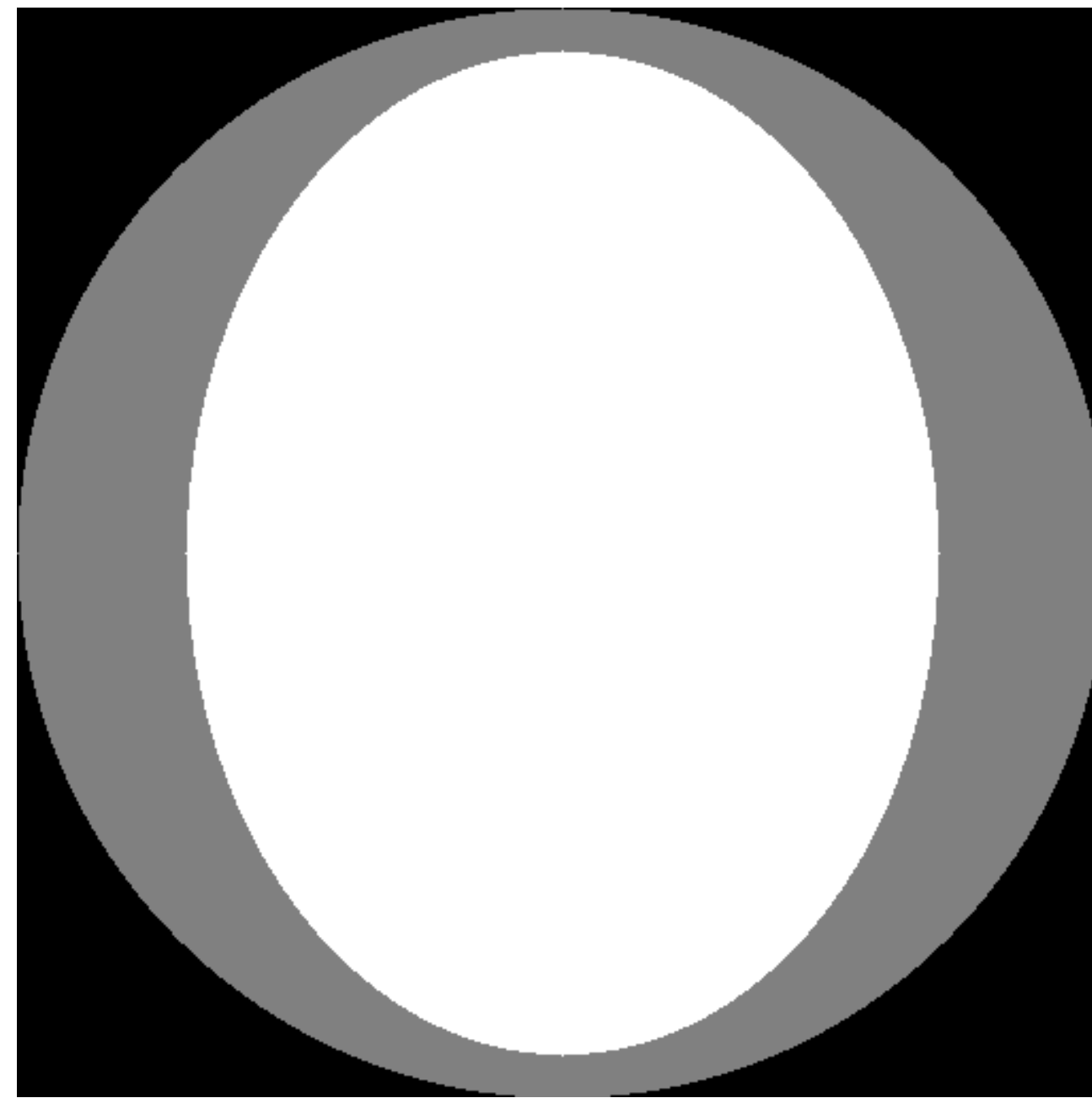
$$\bigcap_{\theta=0}^{\pi} A_{\theta}$$

# Outline

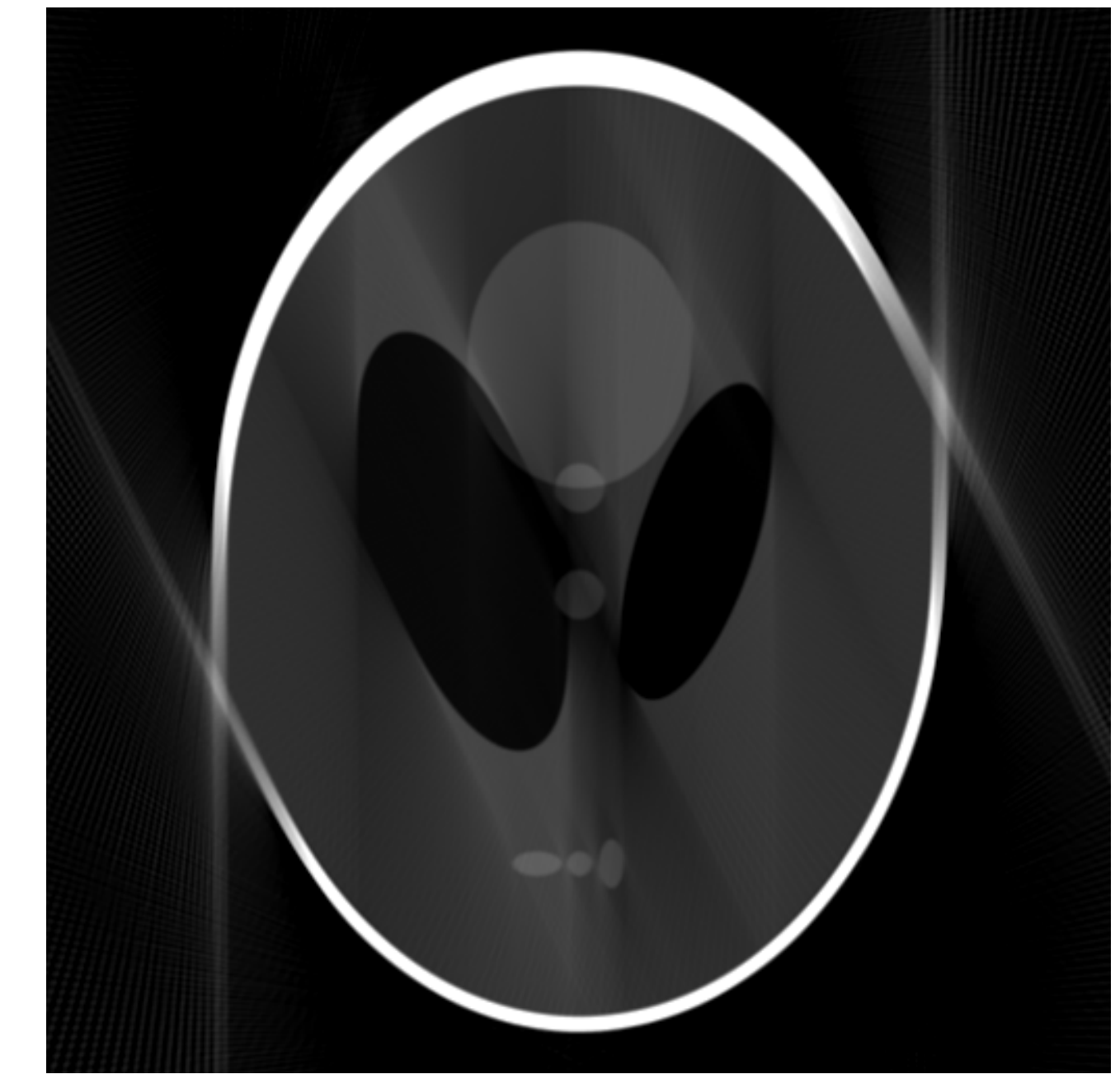
- Background.
- Measurement Model and Mask Reconstruction Algorithms for Known Object Contour.
- Automatic Mask Generation from X-ray CT Sinograms Using a Convex Hull of the Object.
- Numerical Examples
  - Shepp-Logan phantom reconstruction,
  - Industrial object reconstruction.
- Plans for Next Period.



(a)



(b)

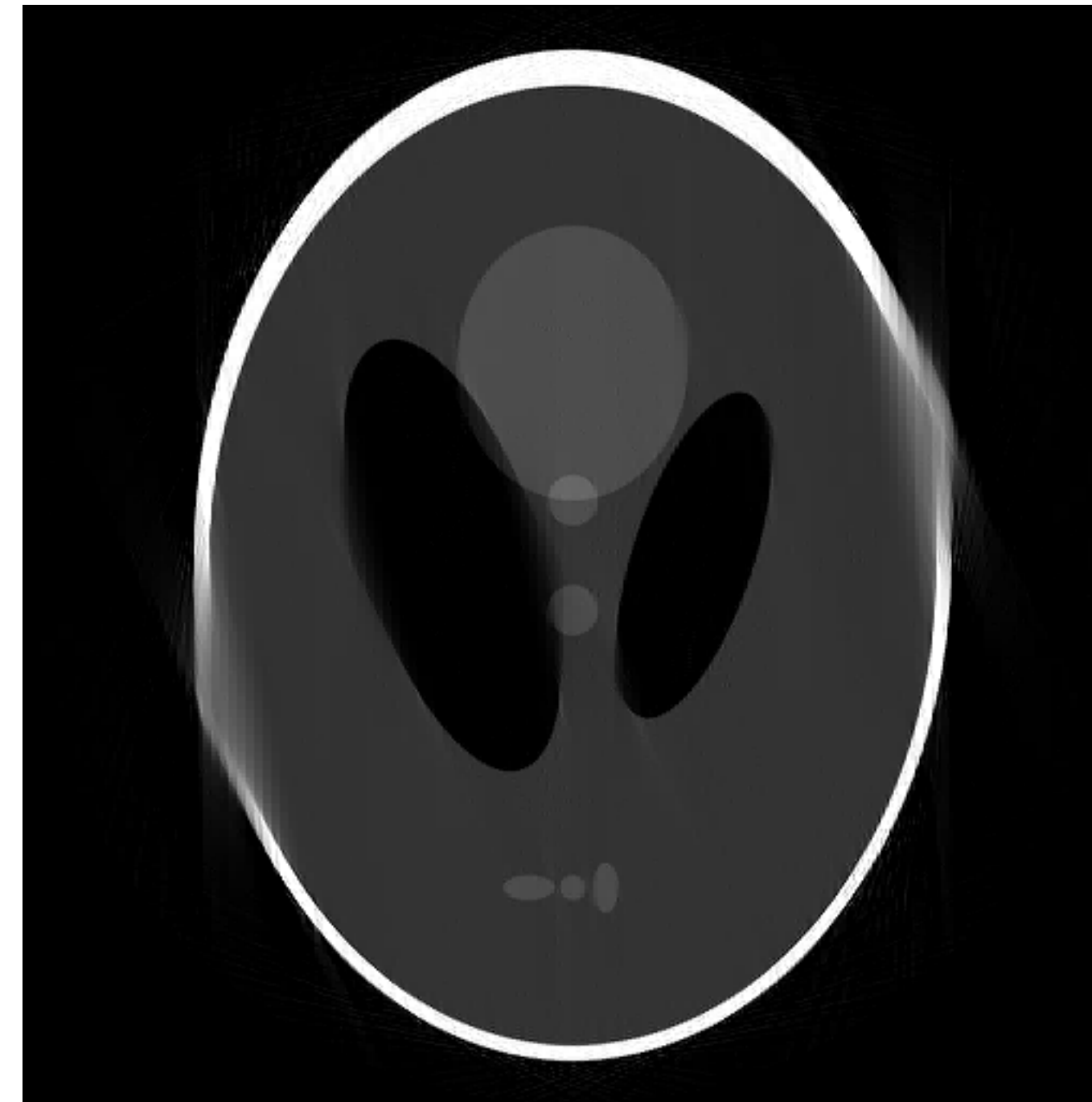


(c)

- (a) 155 limited-angle projections in the 2-D frequency plane,  
(b) full and outer-shell masks of the Shepp-Logan phantom, and  
(c) standard filtered backprojection (FBP) reconstruction (PSNR = 19.9 dB).



(d)



(e)

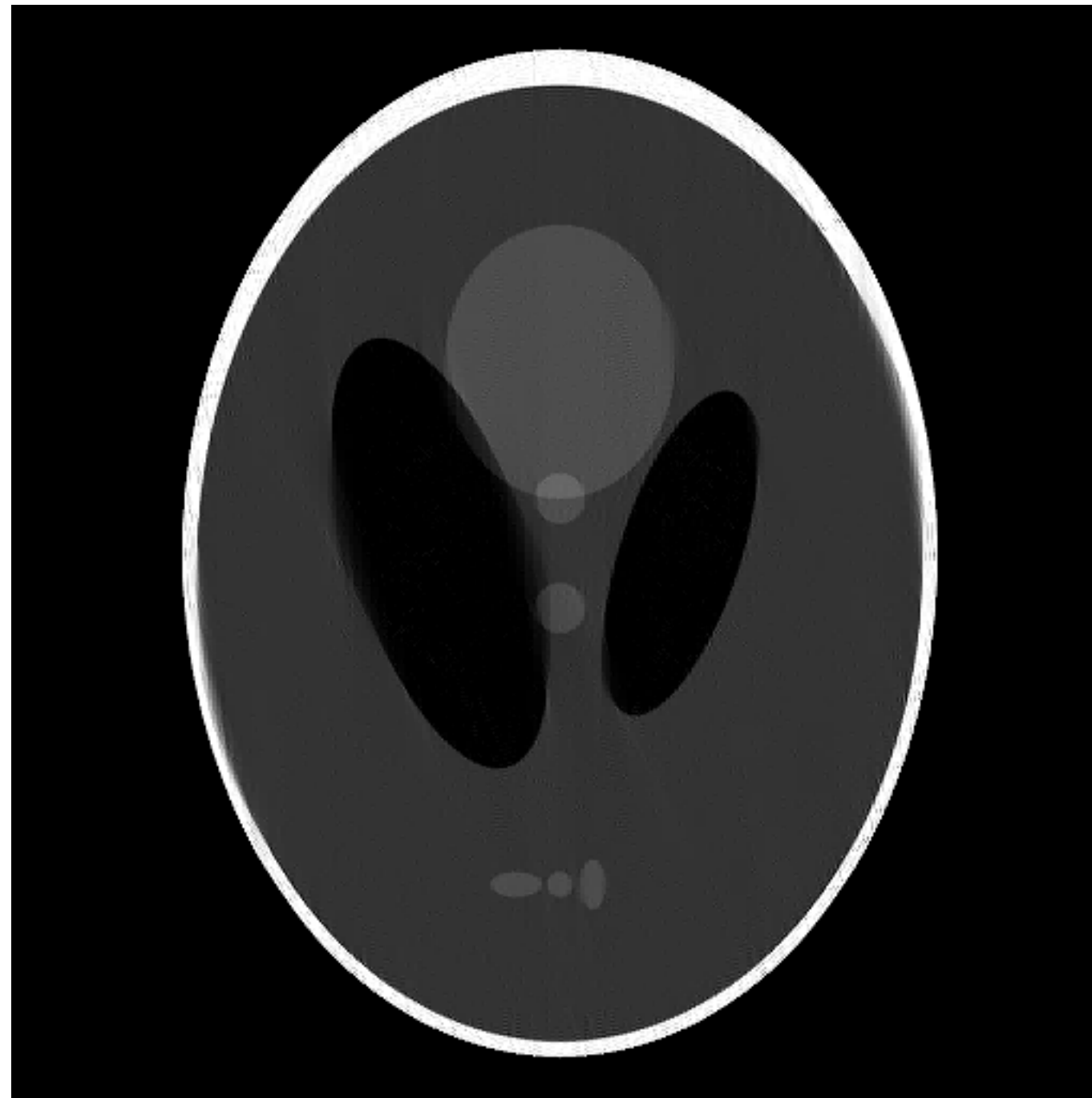


(f)

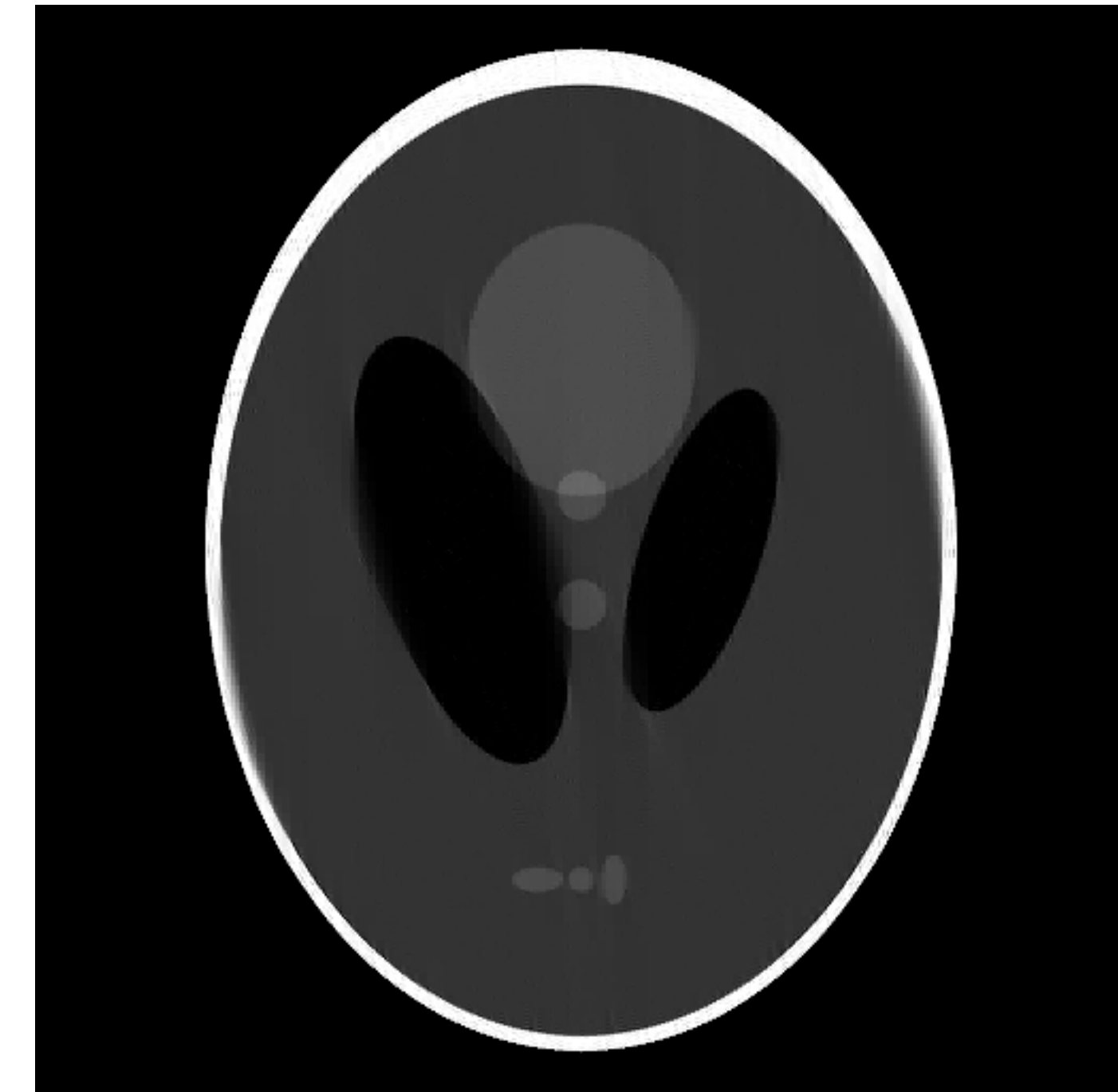
Imposing signal sparsity only: (d) DORE (PSNR = 22.7 dB), (e) GPSR (PSNR = 22.9 dB), (f) FPC<sub>AS</sub> (PSNR = 22.5 dB) reconstructions.



(g)



(h)

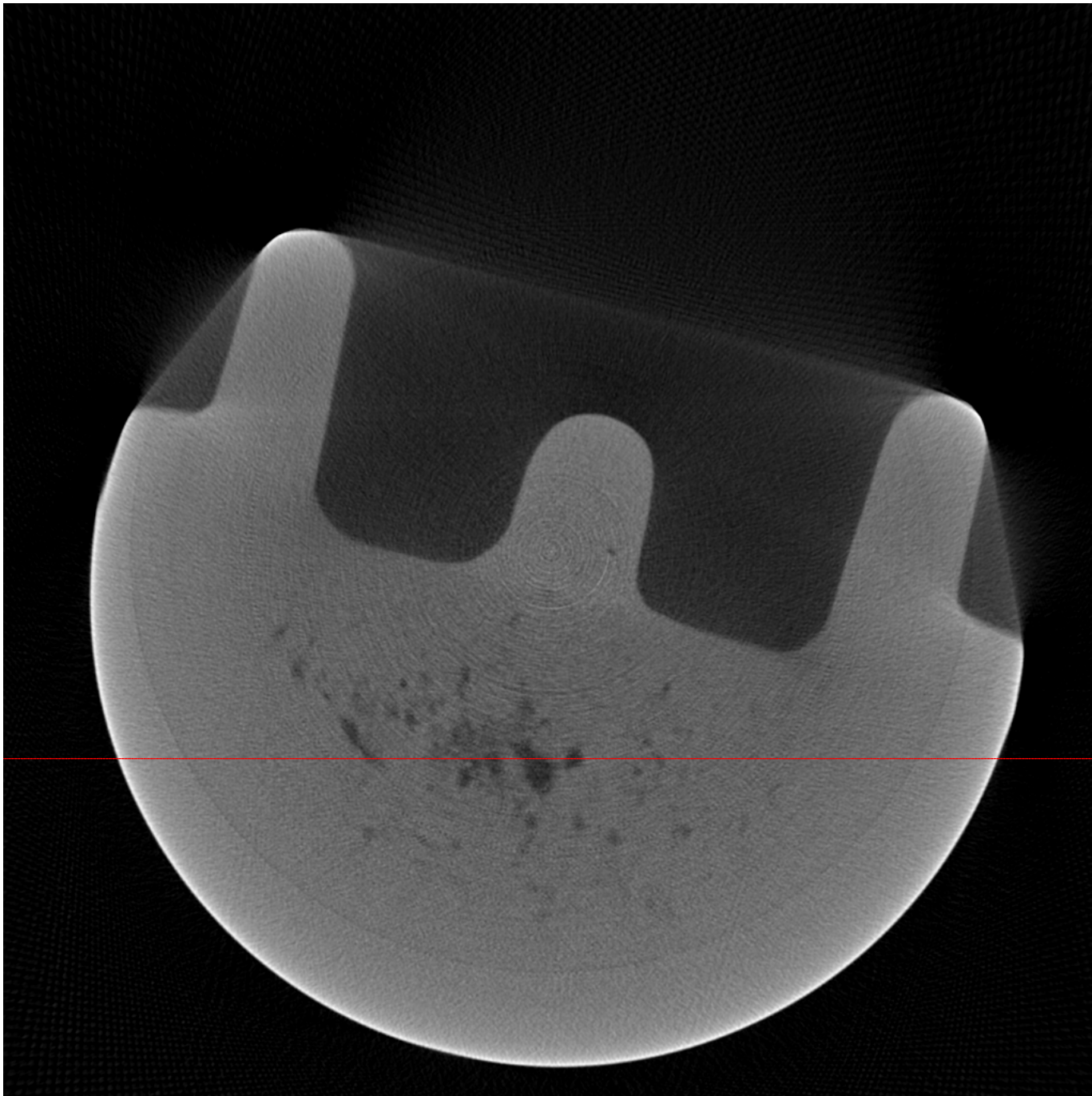


(i)

Imposing both the signal sparsity and geometric object constraints:  
(g) mask DORE (PSNR = 25.8 dB),  
(h) mask GPSR (PSNR = 25.3 dB), and  
(i) mask FPC<sub>AS</sub> (PSNR = 26.4 dB) reconstructions.

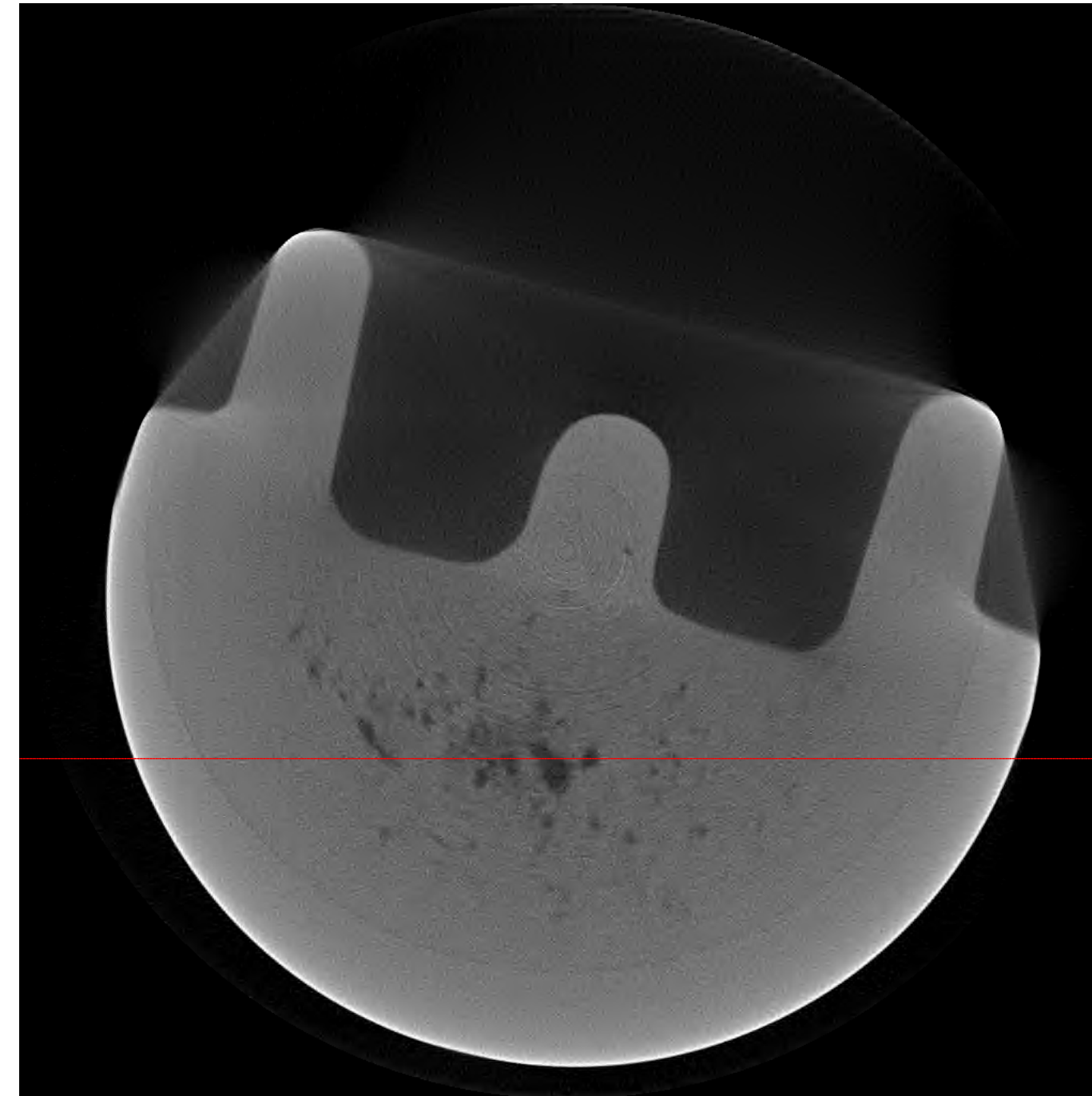
# Outline

- Background.
- Measurement Model and Mask Reconstruction Algorithms for Known Object Contour.
- Automatic Mask Generation from X-ray CT Sinograms Using a Convex Hull of the Object.
- Numerical Examples
  - Shepp-Logan phantom reconstruction,
  - Industrial object reconstruction.
- Plans for Next Period.

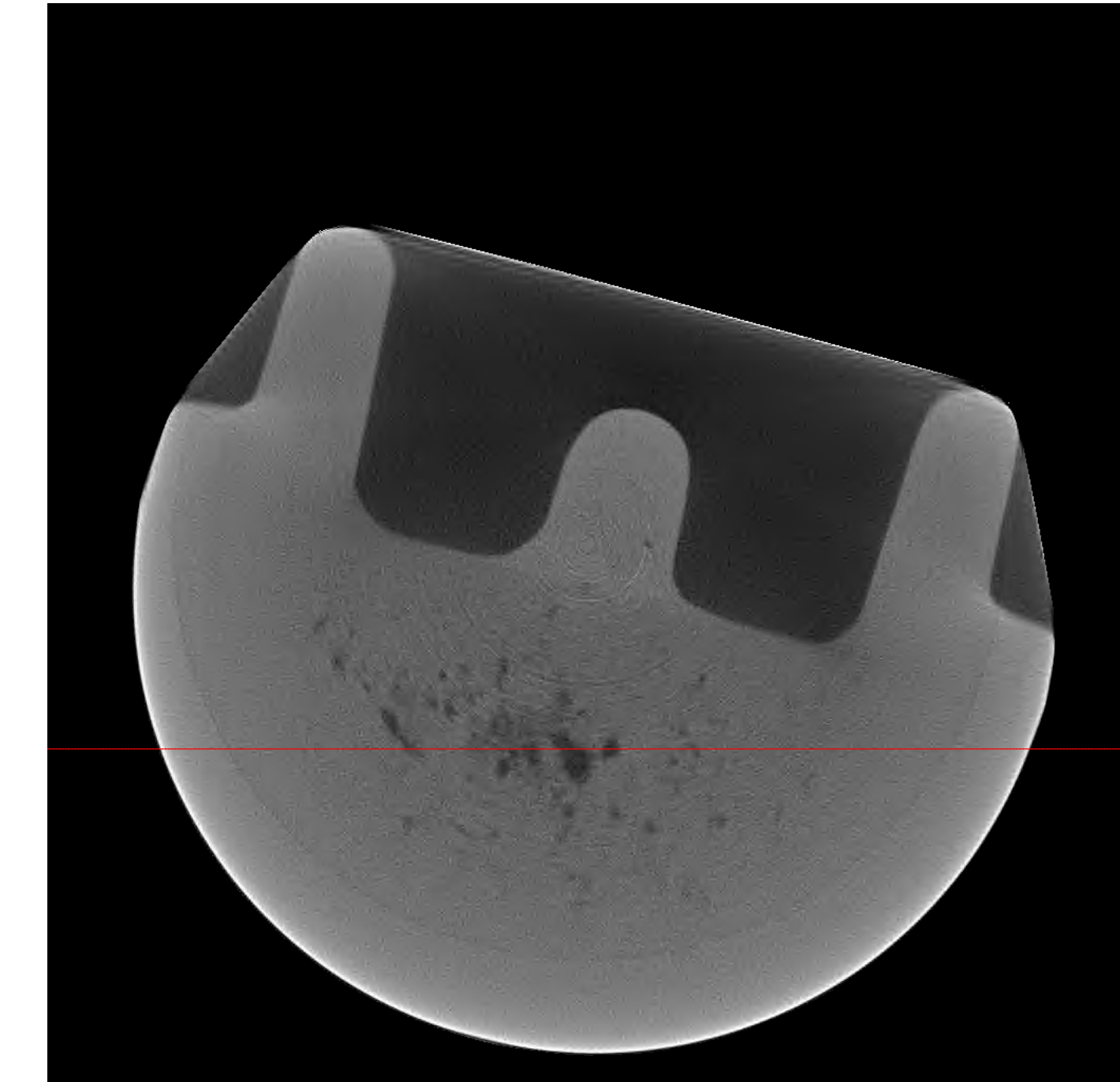


(a)

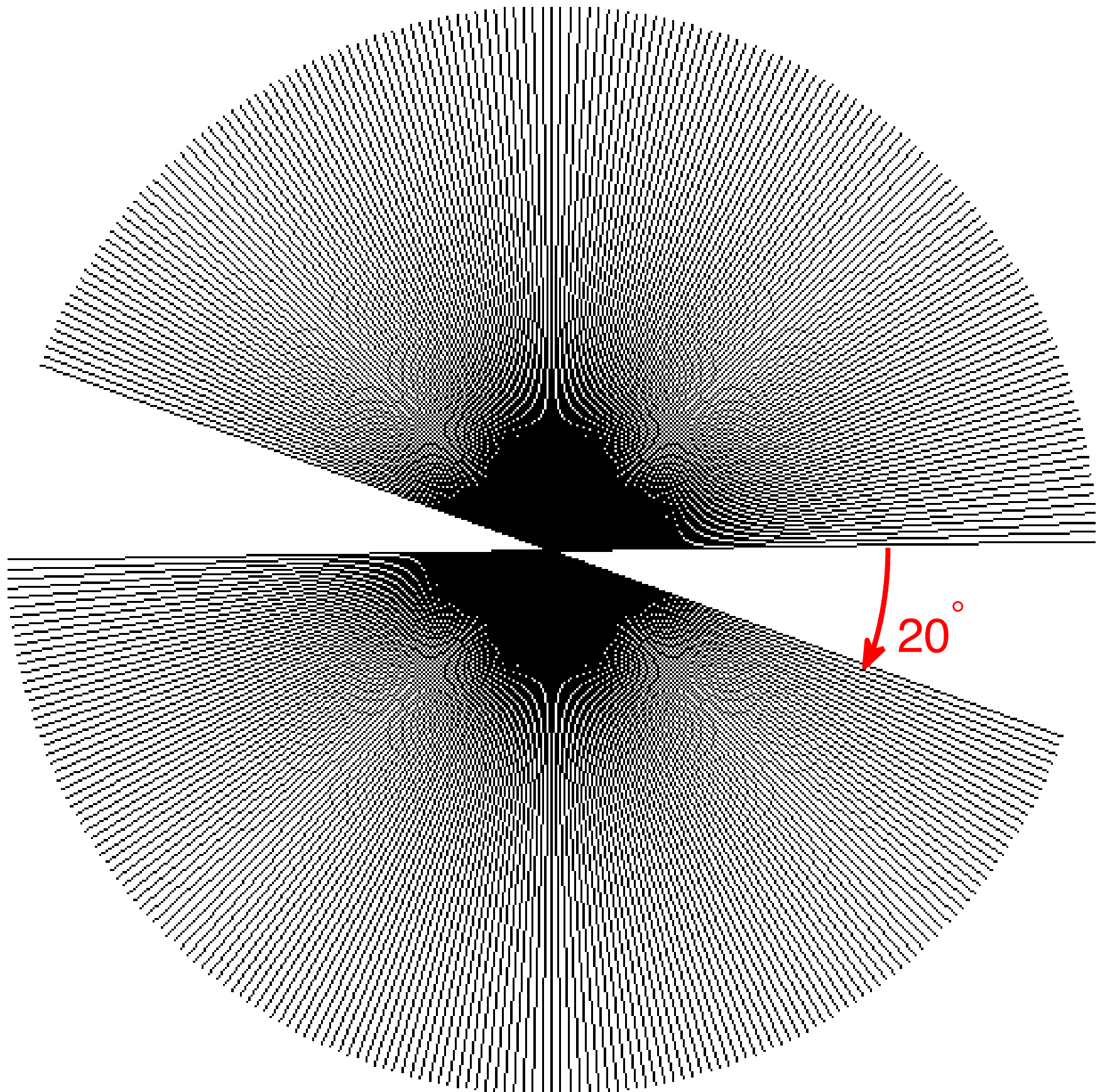
(a) FBP,  
(b) DORE, and  
(c) mask DORE reconstructions from 180 equi-spaced projections,  
where the mask has been constructed from the object's parallel-beam  
sinogram using  $\bigcap_{k=1}^{180} A_{\pi(k-1)} / 180$ .



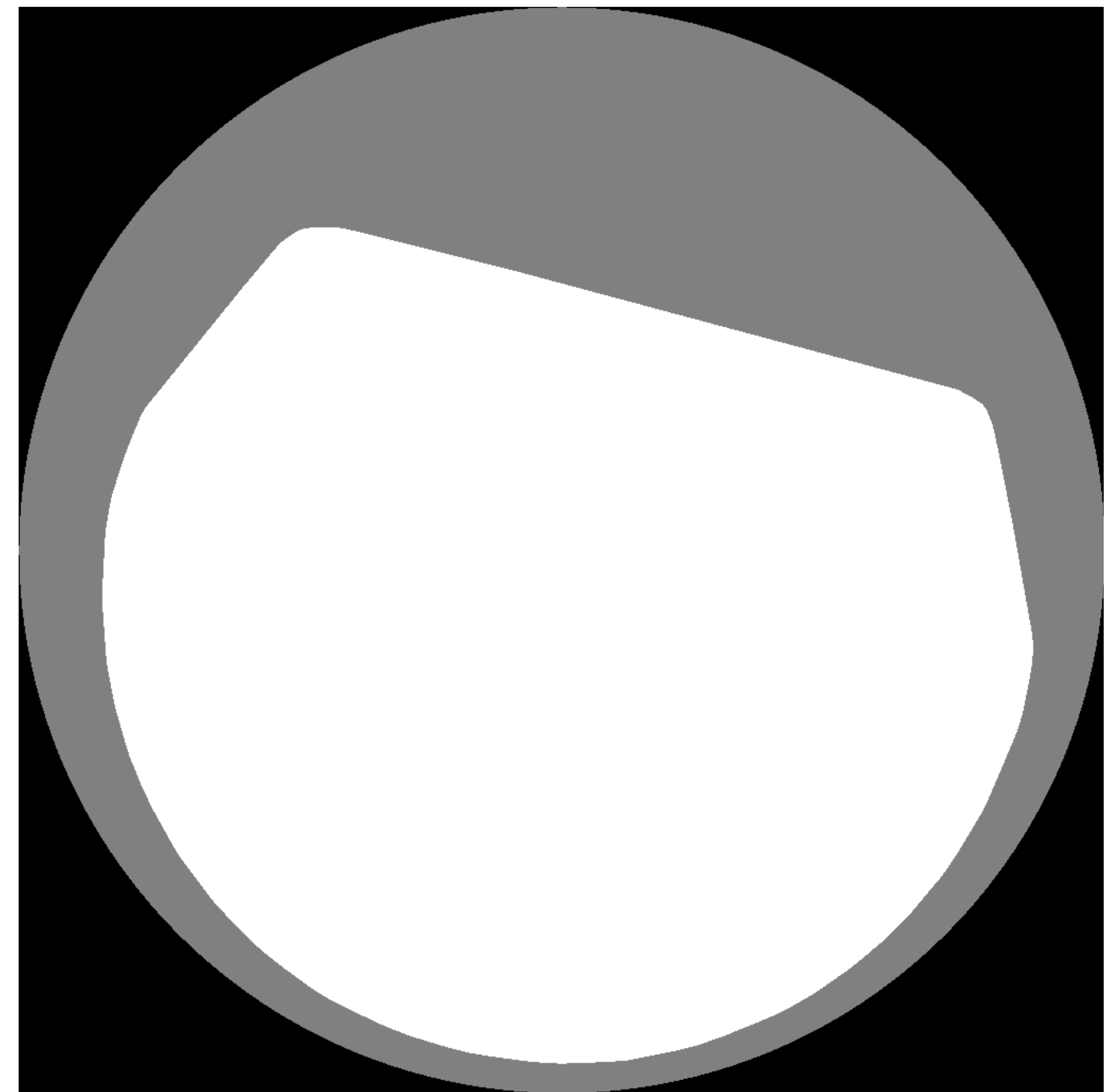
(b)



(c)

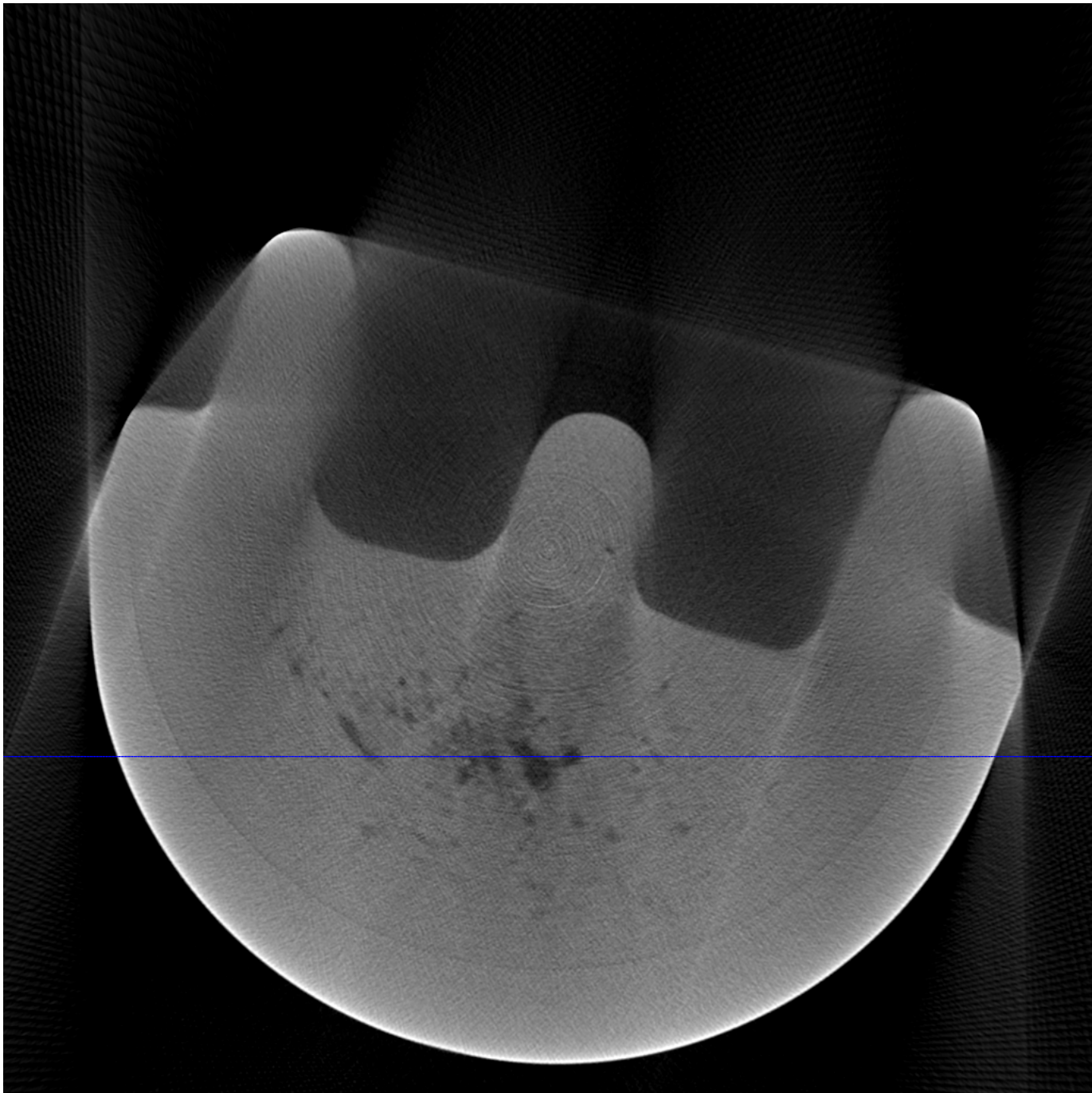


(a)



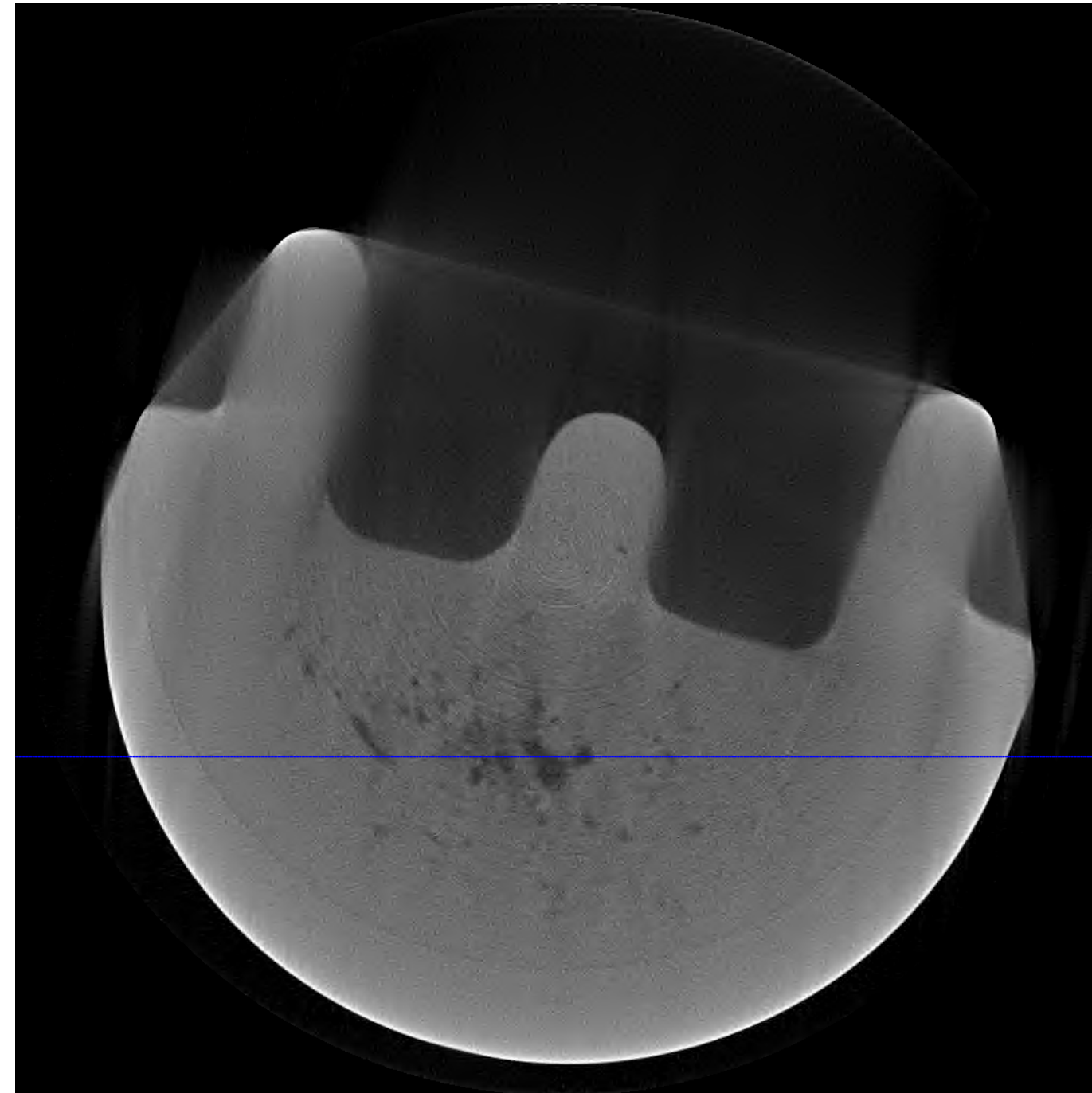
(b)

- (a) 160 limited-angle projections in the 2-D frequency plane and  
(b) full and outer-shell masks of the industrial object.

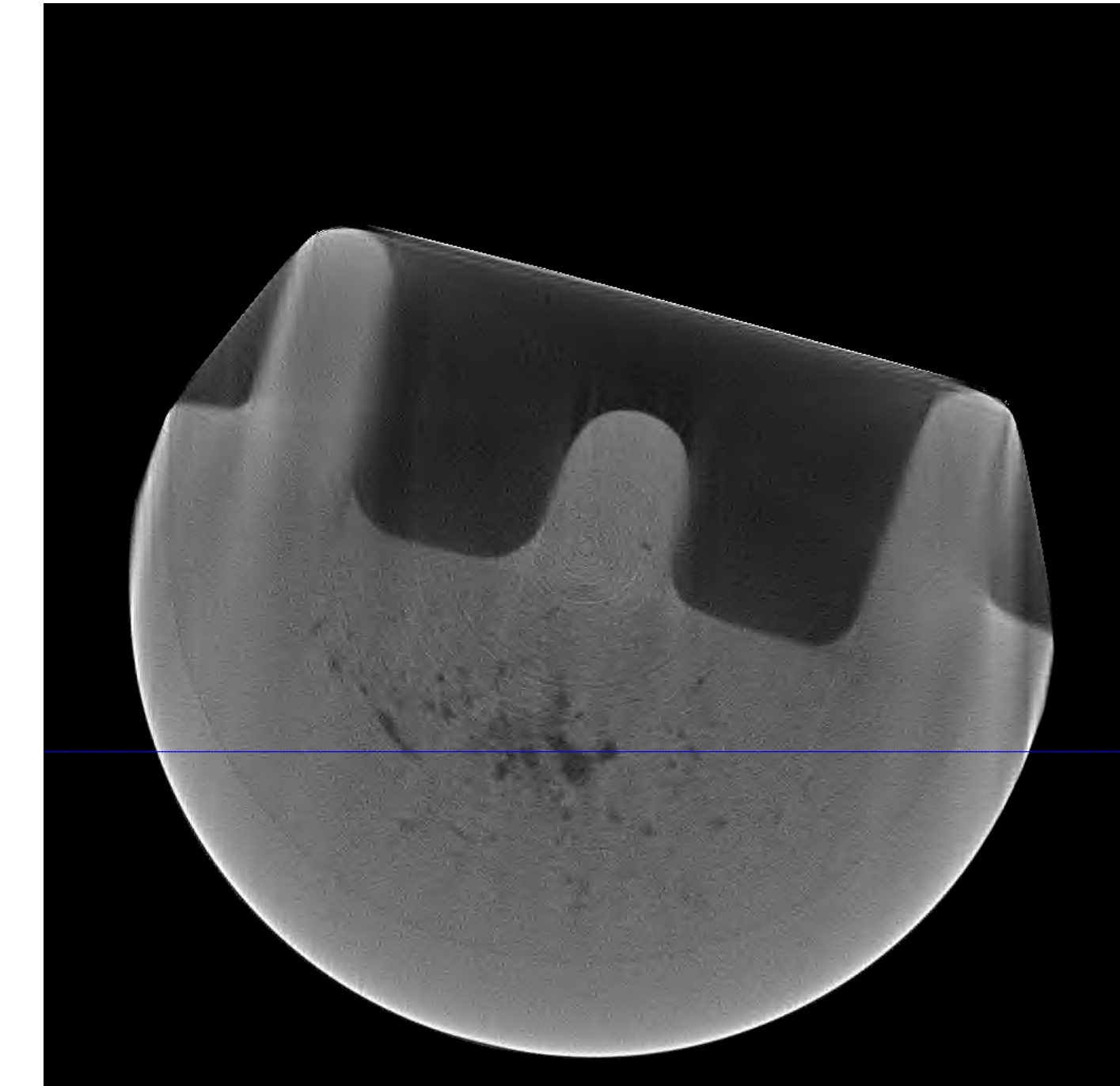


(a)

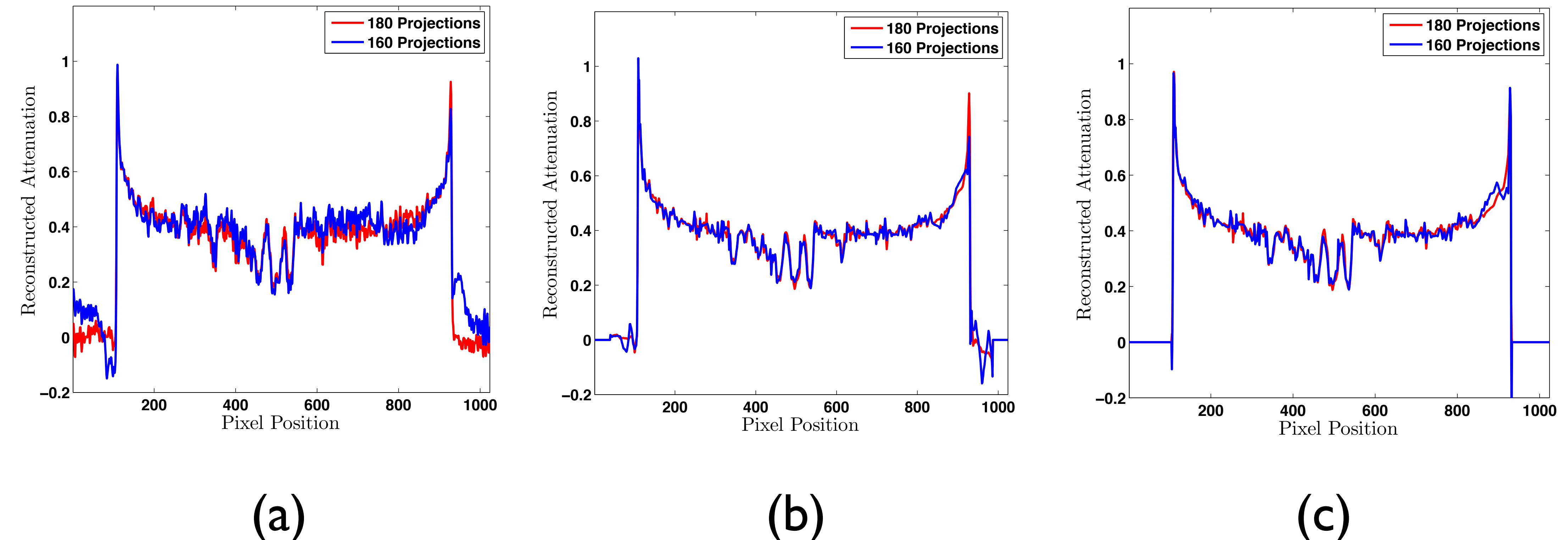
(a) FBP,  
(b) DORE, and  
(c) mask DORE reconstructions from 160 limited-angle projections,  
where the mask has been constructed from the object's parallel-beam  
sinogram using  $\bigcap_{k=1}^{180} A_{\pi(k-1)}/180$ .



(b)



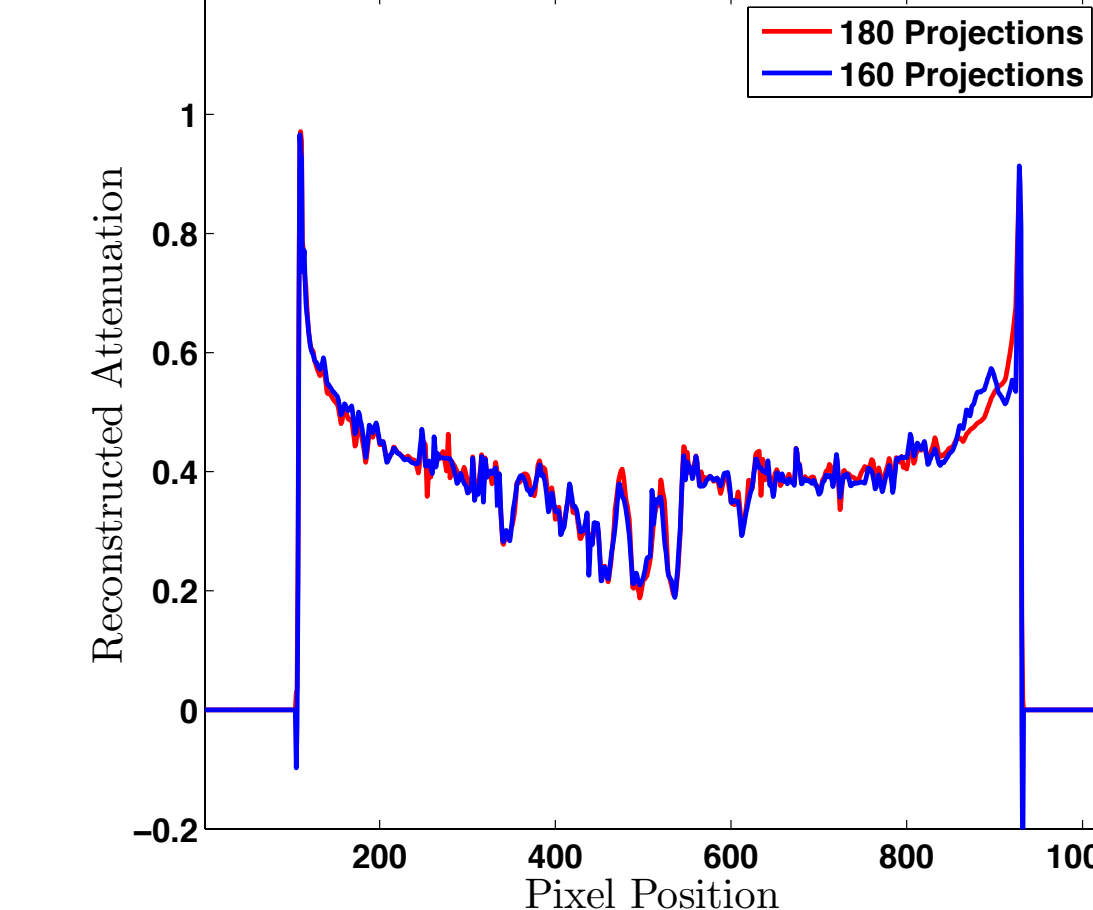
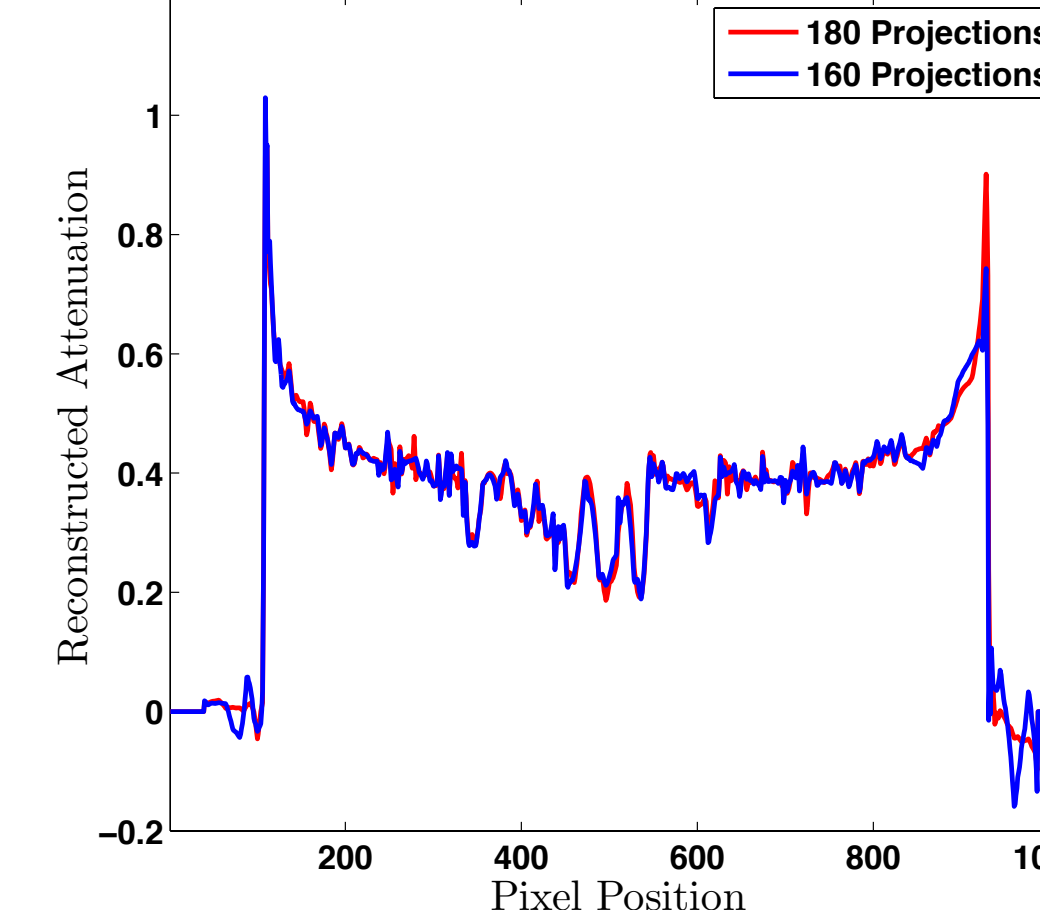
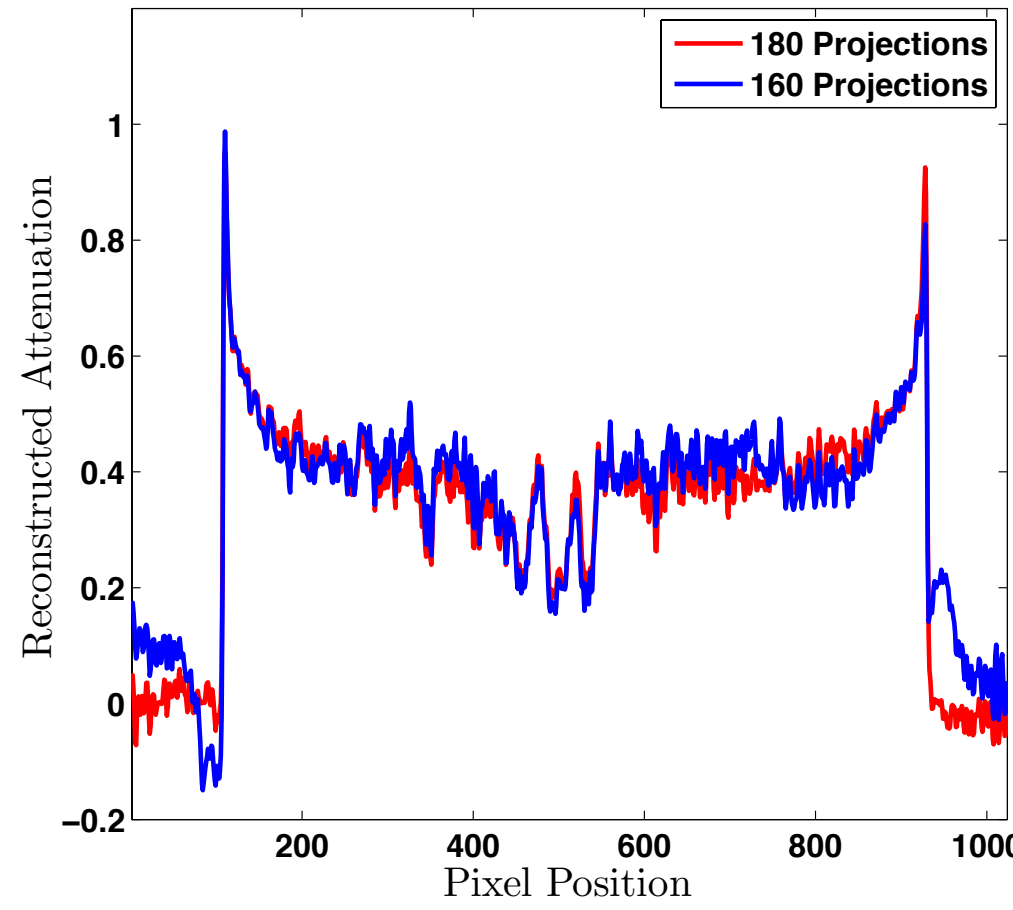
(c)

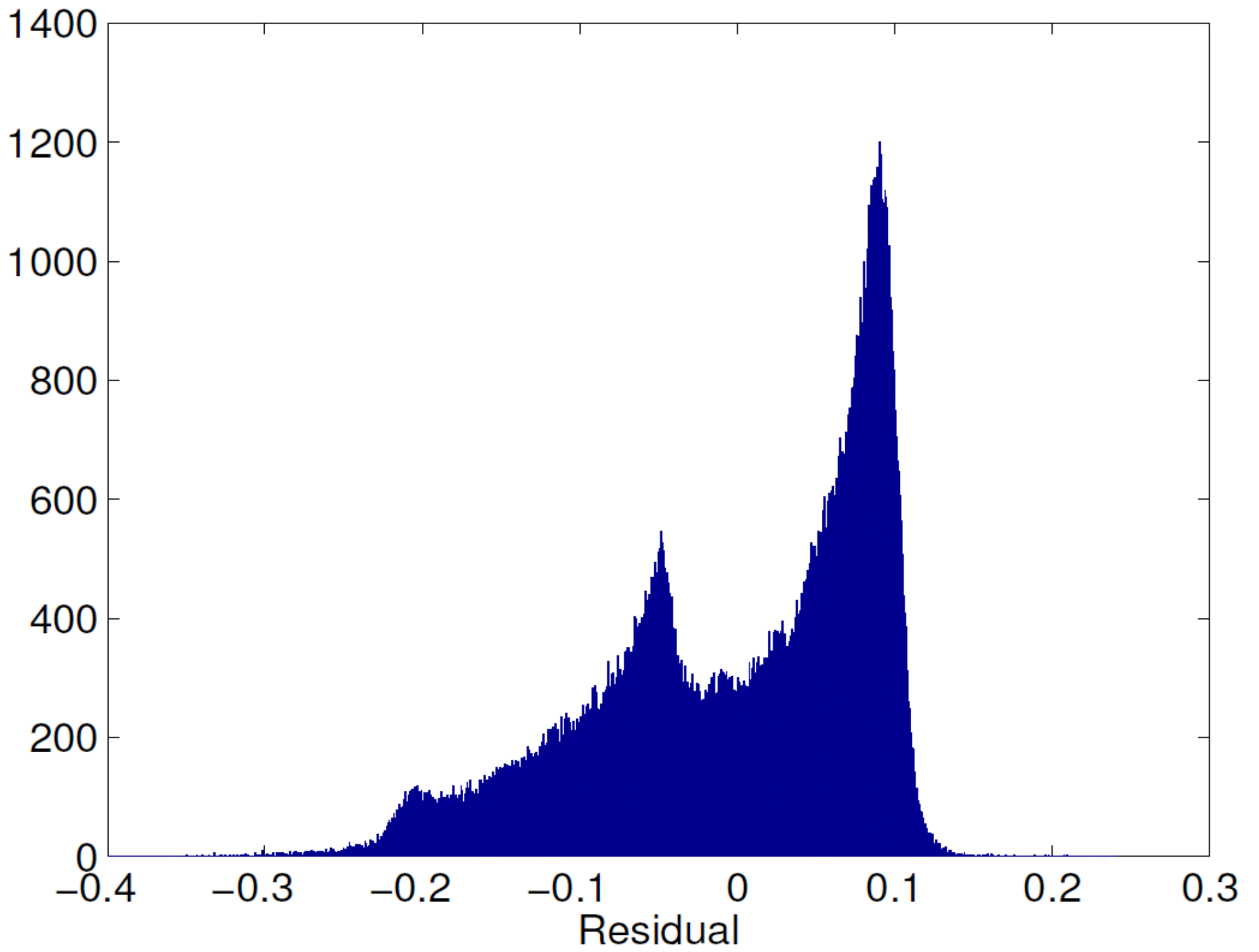


(a) FBP,  
(b) DORE, and  
(c) mask DORE reconstruction profiles.

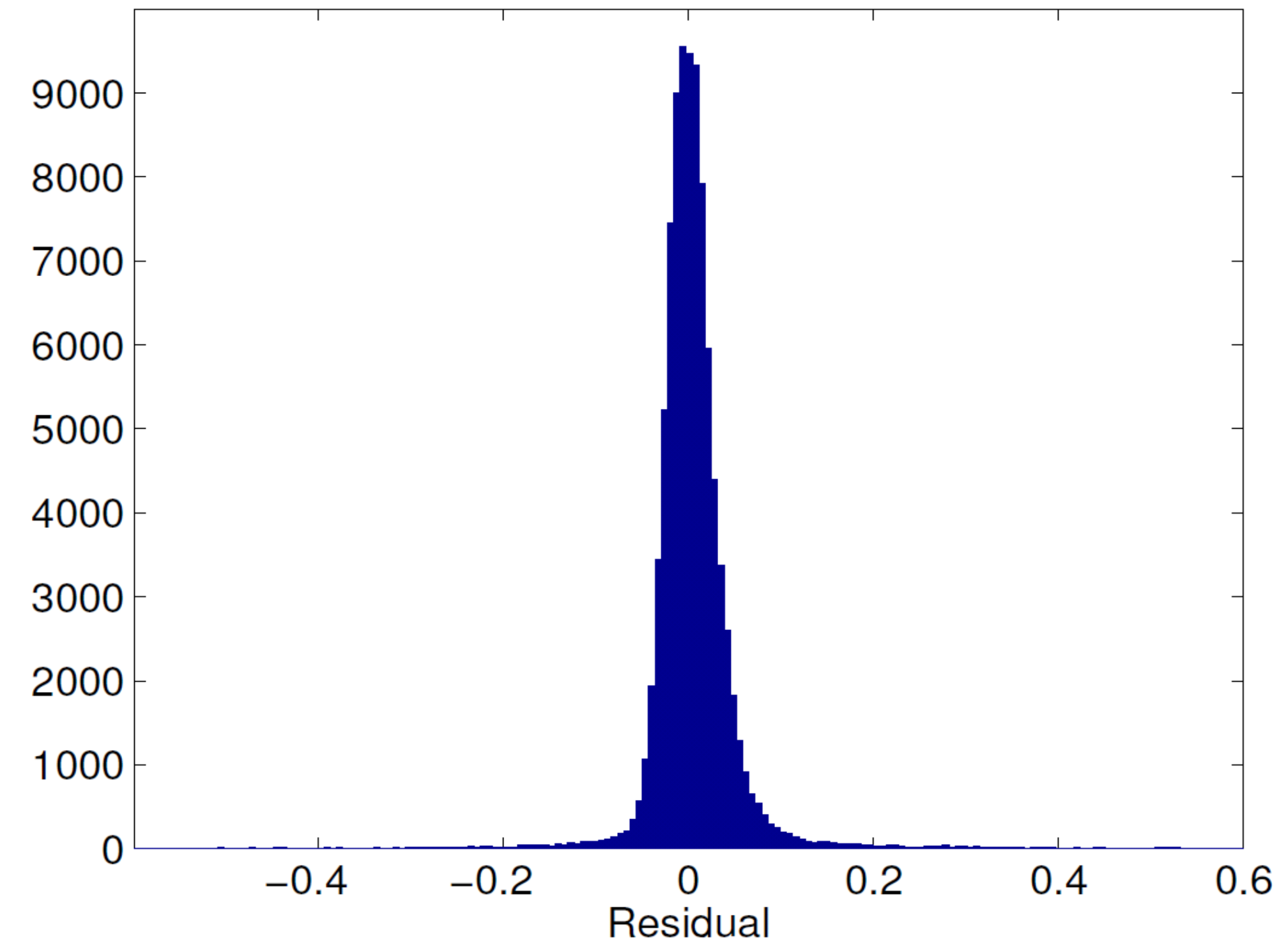
# Plans for Next Period

- We have shown that imposing the signal sparsity and geometric information about the inspected object can improve signal reconstruction from X-ray CT projections.
- However, real NDE X-ray CT data requires further processing. Observe the strong cupping artifacts in all real-data reconstructions, including the standard FBP method:





(a)



(b)

Residual error histograms from FBP reconstructions using 180 uniform-angle projections from (a) real X-ray CT data of an industrial object and (b) simulated X-ray CT data generated from the analytical sinogram of the analog Shepp-Logan phantom.

# Beam Hardening

These artifacts occur because a polychromatic X-ray source is employed for inspection and are caused by the different absorption rates of the photons at different energy levels, which is called the *beam hardening effect*.

The measured projection along a straight line  $l$  defined by

$$p_\theta(t) = -\ln \left( \frac{\int S(E) e^{-\int \mu(x,y,E) dl} dE}{\int S(E) dE} \right)$$

where  $S(E)$  is the energy spectrum of the X-ray source and  $\mu(x,y,E)$  is the attenuation coefficient for a photon with energy  $E$  penetrating the inspected object at position  $(x,y)$ .

# MILESTONES (2012):

March 31:

- Fine-tuned the sensing matrix computations to improve the reconstruction accuracy of our sparse X-ray CT reconstruction algorithms.
- Automated the object contour information extraction by constructing a convex hull of the inspected object directly from the measured sinograms.
- Constructed examples using both realistic simulated and real X-ray CT data to demonstrate the utility of the proposed mask approach.

# MILESTONES (2012, cont.):

March 31:

- Automated the step size selection.
- Applied a tree structure model to exploit signal transform coefficient correlation and designed a signal reconstruction algorithm that takes advantage of this structure.
- Developed a method for sparse signal reconstruction from quantized noisy measurements.

# MILESTONES (2012, cont.):

March 31:

- Automated the step size selection.
- Applied a tree structure model to exploit signal transform coefficient correlation and designed a signal reconstruction algorithm that takes advantage of this structure.
- Developed a method for sparse signal reconstruction from quantized noisy measurements.
- Identified beam hardening phenomenon as an obstacle to further improvement of sparse signal reconstruction in NDE applications of X-ray CT.

# MILESTONES (2012, cont.):

March 31:

- Automated the step size selection.
- Applied a tree structure model to exploit signal transform coefficient correlation and designed a signal reconstruction algorithm that takes advantage of this structure.
- Developed a method for sparse signal reconstruction from quantized noisy measurements.
- Identified beam hardening phenomenon as an obstacle to further improvement of sparse signal reconstruction in NDE applications of X-ray CT.

# MILESTONES (2012, cont.):

Sept. 30:

- Develop beam-hardening correction algorithms.
- Apply our reconstruction algorithm that takes advantage of the signal coefficient tree structure to realistic simulated and real CT data.